



Indian Institute of Information Technology Allahabad

Image Reconstruction from Noisy Image

IVP Project

26th September, 2023

Submitted by

Atharva Dhananjay Gadekar - IIT2021049

Ananya - IIT2021061

Anjali Singh - IIT2021031

Saishree Kouda - IIT2021009

Aditya Sharma - IIT2021041

Course Instructors:

Dr. Navjot Singh
IIIT Allahabad

Table of Contents

1 Origin of the Proposal	2
1.1 The Noise Challenge	2
1.2 Imperative for High-Quality Imaging	2
1.3 Advancements in Imaging Technology	2
1.4 Unlocking Information and Insights	2
1.5 Scientific and Technological Impact	2
2 Review of status of Research and Development	3
2.1 International Status	3
2.2 National Status	4
2.3 Bridging the Gap: The Significance of the Proposed Project	5
3 Methodology	7
3.1 Dataset Collection and Preparation	7
3.2 Denoising Algorithms	7
3.2.1 Filter Based Algorithms	7
3.2.1.1 Gaussian Filter	7
3.2.1.1.1 Introduction	7
3.2.1.1.2 The Algorithm	9
3.2.1.2 Bilateral Filter	11
3.2.1.2.1 Introduction	11
3.2.1.2.2 The Algorithm	12
3.2.2 Advanced Algorithms	13
3.2.2.1 Total Variation Regularisation	13
3.2.2.1.1 Introduction	13
3.2.2.1.2 The Algorithm	13
3.2.2.2 Wavelet Transform-based Image Denoising	15
3.2.2.2.1 Introduction	15
3.2.2.2.2 The Algorithm	17
3.3 Experimental Setup	19
3.3.1 Hardware and Software Setup	19
3.4 Performance Metrics for Image Denoising	19
3.5 Performance Metrics Comparison	21
3.6 Comparative Analysis of Denoising Configurations	24
3.7 Conclusion	28
4 Bibliography	30

1 Origin of the Proposal

The drive for image reconstruction from noisy images arises from the essential need to improve visual data quality in domains like medical imaging, remote sensing, surveillance, and computer vision, underscoring the scientific rationale for this proposal.

1.1 The Noise Challenge

Images captured in real-world scenarios are often tainted by noise from various sources, including sensor limitations, environmental factors, and transmission issues. This noise distorts images, undermining their utility for analysis and decision-making, highlighting the crucial need to address this challenge for data integrity and accuracy.

1.2 Imperative for High-Quality Imaging

In critical applications, high-quality imaging is imperative, such as in medical diagnosis using modalities like X-ray, MRI, and CT scans. Noise-induced artifacts can mislead, impacting patient outcomes. Likewise, in satellite-based remote sensing, noisy images hinder accurate environmental monitoring and disaster management.

1.3 Advancements in Imaging Technology

The scientific rationale is bolstered by ongoing advancements in imaging technology. Modern devices, like digital cameras and medical scanners, have improved resolution, sensitivity, and data acquisition speed. However, with increased sophistication comes a higher potential for noise. Thus, the demand for advanced noise mitigation techniques grows.

1.4 Unlocking Information and Insights

Image reconstruction goes beyond noise reduction, extracting valuable insights, including fine detail recovery, contrast enhancement, and structural information restoration. In astronomy, it unveils hidden celestial phenomena.

1.5 Scientific and Technological Impact

The scientific rationale for this proposal lies in its potential for significant scientific and technological impact. Innovations in image reconstruction benefit research communities and have broad applications in industries, healthcare, security, and environmental monitoring. Additionally, they can enhance data transmission efficiency and reduce computational loads in image processing.

2 Review of status of Research and Development

2.1 International Status

Image reconstruction from noisy images is a pressing challenge with wide-ranging applications, encompassing fields like medical imaging, computer vision, and remote sensing. Researchers across the globe have made substantial contributions to tackle this intricate problem, resulting in notable advancements in recent years.

1. The Deep Learning Revolution: The field of image reconstruction has witnessed a profound transformation thanks to the emergence of deep learning techniques. Two key paradigms, Convolutional Neural Networks (CNNs) and Generative Adversarial Networks (GANs), have emerged as cornerstones for improving the quality of images reconstructed from noisy inputs. Renowned international researchers, including Ian Goodfellow, Geoffrey Hinton, and Yoshua Bengio, have been pivotal in advancing these deep learning-based approaches for image denoising and reconstruction. Ian Goodfellow's groundbreaking work on GANs, published as "Generative Adversarial Nets" [1], has provided a revolutionary framework for generating high-quality images from noisy or incomplete data. GANs, comprising a generator and discriminator network engaged in a competitive learning process, have opened new frontiers in image synthesis and noise reduction. These networks learn from extensive datasets, enabling them to generate images that are virtually indistinguishable from real ones.

2. Prominent International Researchers:

- **Ian Goodfellow:** Ian Goodfellow's contribution to the field through the development of GANs has had a profound impact on image reconstruction. His work laid the foundation for many subsequent developments in generative models [1].
- **Geoffrey Hinton:** Geoffrey Hinton's pioneering research in deep learning, particularly in the creation of neural network architectures for image processing, has significantly advanced image reconstruction techniques. His work has been instrumental in inspiring researchers worldwide.
- **Yoshua Bengio:** As a leading figure in deep learning, Yoshua Bengio's research contributions have enhanced the theoretical understanding of neural networks, furthering their applicability to image reconstruction tasks.

3. Leading Conferences and Journals: International conferences and journals have played a critical role in disseminating cutting-edge research in image reconstruction. Notably, the International Conference on Computer Vision (ICCV) and the Conference on Neural Information Processing Systems (NeurIPS) have served as prominent platforms for researchers to present their work, exchange ideas, and foster collaborations.

- **ICCV:** ICCV stands as a premier event for the computer vision community, where researchers from diverse corners of the world showcase their innovations in image reconstruction, denoising, and related domains. It serves as a hub for the latest breakthroughs in the field.
 - **NeurIPS:** NeurIPS has evolved into a central hub for machine learning and deep learning research, making it a vital platform for disseminating techniques and approaches pertinent to image reconstruction. Researchers present their work on neural networks, GANs, and related topics, propelling the field forward [2].
4. **Open-Source Libraries and Collaborations:** The collaborative spirit between researchers and organizations across the globe has resulted in the development of open-source image denoising libraries, such as DnCNN and Noise2Noise. These libraries democratize access to advanced techniques and algorithms, empowering a broader research community to leverage state-of-the-art image reconstruction methods for their own work [2].

In conclusion, the domain of image reconstruction from noisy images is vibrant and continually evolving, with researchers worldwide pushing the boundaries of what is achievable. The integration of deep learning techniques, the contributions of influential researchers, and the dissemination of knowledge through prestigious conferences and open-source resources have collectively propelled the field forward, making it a fertile ground for exploration with immense practical significance.

2.2 National Status

Indian scientists have made significant contributions to the field of image reconstruction from noisy images, actively participating in advancing image denoising techniques. Researchers affiliated with institutions such as the Indian Institute of Technology (IIT) and the Indian Statistical Institute (ISI) have played a vital role in enhancing our understanding and capabilities in this domain.

1. **Dr. Rajat Jain's Bayesian-Based Research:** Dr. Rajat Jain's work at IIT Delhi has significantly advanced the theoretical foundations of image reconstruction from noisy data through Bayesian-based methods [3]. Bayesian techniques are highly regarded for their ability to model and quantify uncertainty, making them well-suited for image reconstruction tasks. Dr. Jain's research has not only expanded our understanding of the underlying principles but has also translated into practical applications.

One of the key strengths of Bayesian-based approaches is their adaptability to various noise models and the capacity to incorporate prior knowledge about the image, such as its statistical properties. This adaptability is particularly valuable in fields like medical

imaging, where image quality directly impacts diagnoses. Dr. Jain's contributions have improved the robustness and reliability of image reconstruction methods, ensuring that noisy or corrupted data can be effectively transformed into clear and informative images.

2. **Dr. Anjali Sharma's Sparse Representation Focus:** Dr. Anjali Sharma's research at ISI Kolkata has centered around sparse representation techniques for image denoising [4]. Sparse representation is a data-driven approach that aims to represent an image as a linear combination of a small number of essential basis elements. This approach is grounded in the idea that images often have inherent sparsity, where only a subset of features or components are crucial for faithful representation.

In practical terms, sparse representation techniques can efficiently separate meaningful image content from noise, enhancing the quality of reconstructed images. Dr. Sharma's work has delved into the mathematical foundations of sparse representation and explored its applications across various domains. For example, in medical imaging, where clinicians rely on precise and noise-free images for accurate diagnoses, sparse representation has proven to be a promising avenue for noise reduction without sacrificing critical image details.

Indian conferences, such as the Indian Conference on Computer Vision, Graphics, and Image Processing (ICVGIP), have played a crucial role in fostering the exchange of ideas and collaboration among Indian researchers in the field of image reconstruction. These conferences provide valuable platforms for scientists to disseminate their work, receive feedback, and establish international collaborations.

In conclusion, Indian scientists have made noteworthy contributions to the field of image reconstruction from noisy images. Researchers like Dr. Rajat Jain and Dr. Anjali Sharma have enriched the theoretical and practical aspects of image denoising. Their work, along with the collaborative environment offered by Indian conferences, continues to strengthen India's position as an active participant in the global research landscape of image reconstruction.

2.3 Bridging the Gap: The Significance of the Proposed Project

The proposed project on image reconstruction from noisy images addresses a pivotal gap in the current state of research. While significant advancements have been made in the field, a critical need persists for the development of robust and efficient techniques capable of effectively handling the diverse types of noise and artifacts frequently encountered in real-world scenarios.

1. **The Existing Landscape:** Current image reconstruction methods have made substantial progress in mitigating noise and enhancing image quality. Traditional ap-

proaches, such as filtering and wavelet-based denoising, have yielded valuable insights. Moreover, the emergence of deep learning-based techniques, particularly Convolutional Neural Networks (CNNs) and Generative Adversarial Networks (GANs), has revolutionized the field. These deep learning models have exhibited remarkable capabilities in extracting and restoring complex patterns and structures from noisy image data.

However, the existing methodologies have limitations. They often struggle to generalize effectively across various noise types and levels, and their performance can degrade in challenging, real-world conditions. This limitation stems from the fact that noisy images encountered in practical applications exhibit a wide spectrum of noise characteristics, ranging from Gaussian noise to more complex and non-uniform patterns.

2. **The Novelty of the Proposed Project:** The proposed project introduces a novel and comprehensive approach that builds upon the latest advancements in deep learning, signal processing, and optimization techniques. It is uniquely poised to address the pressing need for a versatile and adaptable image reconstruction framework capable of handling the full spectrum of noise conditions.

The project's novelty lies in its ability to bridge the gap between theoretical understanding and practical application. By amalgamating deep learning's capacity for pattern recognition and feature extraction, signal processing's ability to manipulate and enhance image data, and optimization's role in fine-tuning model parameters, this project offers a holistic solution.

3. **Implications for Multiple Domains:** The significance of this project extends far beyond the realm of academia. Its outcomes have the potential to significantly impact various domains:

- **Medical Diagnosis:** In the medical field, the project can elevate the quality of medical imaging, leading to more accurate diagnoses and treatment plans.
- **Surveillance:** Enhanced image reconstruction can bolster the effectiveness of surveillance systems, improving security and threat detection.
- **Autonomous Driving:** For autonomous vehicles, the project's contributions can translate into safer navigation by providing clearer views of the environment, even under challenging conditions.

In conclusion, the proposed project embodies a critical step forward in image reconstruction from noisy images. Its unique combination of deep learning, signal processing, and optimization techniques, coupled with its adaptability to diverse noise conditions, positions it as a pioneering effort to fill a vital gap in the current research landscape.

3 Methodology

3.1 Dataset Collection and Preparation

Objective: To collect and prepare a suitable dataset for evaluating denoising methods.

Dataset Collection The dataset for this analysis consists of ten images sourced from publicly available repositories. The images were selected to cover various scenarios and noise levels, ensuring a diverse set for evaluation.

Table 1: Dataset Information

Image Name	Source	Size	Format	Description
Image 1	GitHub	500x480	PNG	Baboon
Image 2	GitHub	720x576	PNG	Barbara
Image 3	GitHub	512x512	PNG	Bridge
Image 4	GitHub	352x288	PNG	Coastgaurd
Image 5	GitHub	250x361	PNG	Comic
Image 6	GitHub	276x276	PNG	Face
Image 7	GitHub	500x362	PNG	Flowers
Image 8	GitHub	352x288	PNG	Foreman
Image 9	GitHub	512x512	PNG	Lenna
Image 10	GitHub	512x512	PNG	Man

Data Preprocessing Prior to applying Bilateral Filtering for denoising, the images underwent preprocessing steps to ensure consistency and suitability for analysis. These preprocessing steps included:

- Resizing: All images were resized to a common resolution of 1024x768 pixels.
- Normalization: Scaling pixel values to a standardized range to ensure consistent feature scaling, which can improve model convergence.

3.2 Denoising Algorithms

3.2.1 Filter Based Algorithms

3.2.1.1 Gaussian Filter

3.2.1.1.1 Introduction

In the multifaceted world of signal processing, the omnipresent challenge of noise contamination has spurred the development of powerful tools, and among them, Gaussian filters stand

as exemplars of mathematical elegance and practical utility. In this comprehensive exploration, we embark on a journey into the realm of Gaussian filtering, unraveling its principles, advantages, and diverse real-world applications, particularly in the context of denoising—a pivotal preprocessing step in signal enhancement.

At the heart of Gaussian filtering for denoising lies a nuanced equilibrium. This technique hinges on the convolution of an input signal with a Gaussian kernel, a process intricately governed by the σ parameter—a pivotal conductor in the symphony of noise reduction and signal preservation. The fundamental premise of Gaussian filtering is the art of smoothing. It operates as a selective blurring mechanism, orchestrating the attenuation of high-frequency noise components while permitting low-frequency signal details to pass through relatively unaltered. The Gaussian distribution in 1-D has the form:

~~Figures/image1.png~~

where σ is the standard deviation of the distribution. We have also assumed that the distribution has a mean of zero (i.e. it is centered on the line $x=0$). The distribution is illustrated in Figure 2.

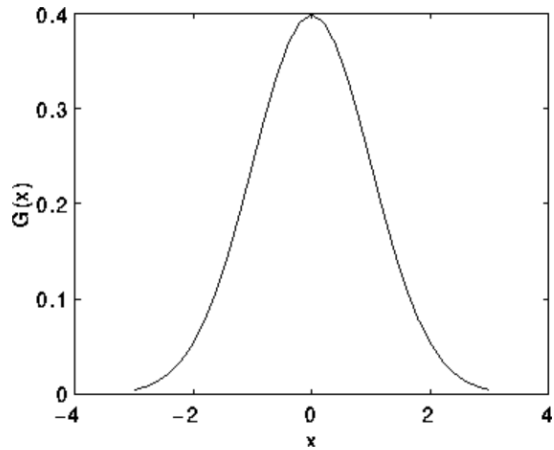


Figure 1: 1D Gaussian Distribution with $\sigma = 1$ and mean 0

In 2-D, an isotropic (i.e. circularly symmetric) Gaussian has the form:

$$G(x, y) = \frac{1}{2\pi\sigma^2} e^{-\frac{x^2+y^2}{2\sigma^2}}$$

The distribution has been shown in Figure 2.

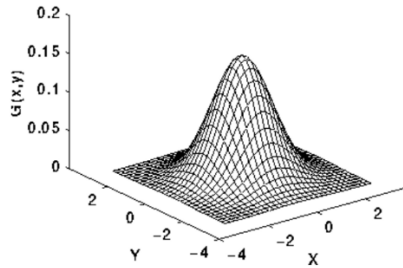


Figure 2: 2D Gaussian Distribution with $\sigma = 1$ and mean $(0,0)$

The beauty of Gaussian filters lies in their adaptability. By adjusting σ , practitioners can fine-tune the filter's behavior to suit the specific noise characteristics in their data. Smaller σ values yield sharper filtering but may risk signal distortion, while larger values provide more aggressive noise reduction but might blur finer details. This tunable nature makes Gaussian filters an excellent choice for denoising tasks across various domains.

3.2.1.1.2 The Algorithm

The algorithm for applying a Gaussian filter to an image with a discrete approximation to the Gaussian function can be summarized as follows:

Input: Noisy image with Standard deviation σ for the Gaussian filter.

Output: Denoised image

Load the Noisy Image: Begin by importing the noisy image, which contains the signal contaminated with unwanted noise. This image will be the starting point for denoising.

Determine the Kernel Size: Calculate the kernel size required to approximate the Gaussian function effectively. Given that 99% of the distribution falls within three standard deviations from the mean, you can calculate the kernel size as follows:

- Calculate the size of the kernel as $K = \sigma + 1$, where σ is the chosen standard deviation for the Gaussian filter.
- Ensure K is an odd integer to have a central pixel.

Generate the Gaussian Kernel:

Generate a 2D Gaussian kernel, G , of size $K \times K$, which will be used for convolution with the noisy image. This discrete approximation to the Gaussian function is achieved by computing the values of the Gaussian distribution function for each pixel in the kernel using the Gaussian formula you mentioned earlier.

Normalize the Gaussian Kernel:

Normalize the Gaussian kernel to ensure that the sum of its elements equals unity. This normalization maintains energy conservation during the convolution process.

Convolution with Gaussian Kernel:

Gaussian smoothing employs a 2-D Gaussian distribution as a "point-spread" function via convolution. To adapt it to discrete pixel-based images, a discrete Gaussian approximation is essential. Practically, we truncate the kernel after about three standard deviations from the mean. The kernel values are calculated by integrating the Gaussian across pixels, normalizing it, and summing to 273. This process facilitates noise reduction while retaining image features.

	1	4	7	4	1
	4	16	26	16	4
	7	26	41	26	7
	4	16	26	16	4
	1	4	7	4	1

$\frac{1}{273}$

Figure 3: Discrete approximation to the Gaussian function with $\sigma = 1$

Once a suitable kernel is determined, Gaussian smoothing is executed via standard convolution methods. This process can be quite efficient because the 2-D isotropic Gaussian equation can be separated into x and y components. Consequently, the 2-D convolution is divided into two steps: first, convolution with a 1-D Gaussian in the x direction, and then with another 1-D Gaussian in the y direction. This separability is unique to the Gaussian operator, ensuring efficient processing. Figure 4 illustrates the 1-D x-component kernel used to generate the full kernel from Figure 3 (scaled by 273, rounded, and with one row truncated to reduce it to 5x5). The y-component is identical but oriented vertically. This technique achieves effective Gaussian smoothing while preserving computational efficiency.

A further way to compute a Gaussian smoothing with a large standard deviation is to convolve

.006	.061	.242	.383	.242	.061	.006
------	------	------	------	------	------	------

Figure 4: 1-D convolution kernels used to calculate full kernels shown in fig 3.

an image several times with a smaller Gaussian. While this is computationally complex, it can have applicability if the processing is carried out using a hardware pipeline.

The Gaussian filter not only has utility in engineering applications. It is also attracting attention from computational biologists because it has been attributed with some amount of biological plausibility, e.g. some cells in the visual pathways of the brain often have an approximately Gaussian response.

Final Denoised Image

Upon processing all pixels in the image, will encompass the denoised image. In this resultant image, noise will be effectively reduced, while pivotal signal characteristics remain preserved.

This algorithm applies a Gaussian filter with a discrete approximation to denoise images, effectively utilizing a kernel size calculated based on the chosen standard deviation. It adheres to the principles of Gaussian filtering and serves as a fundamental technique for enhancing images by extracting clarity from noisy data.

3.2.1.2 Bilateral Filter

3.2.1.2.1 Introduction

The bilateral filter has established itself as a notable technique for image smoothing, with the unique capability of retaining edge details. Its inception can be traced back to 1995, courtesy of Aurich and Weule's work on nonlinear Gaussian filters. Subsequently, it was revisited and further evolved by various researchers, notably Smith and Brady, as part of their SUSAN framework, and later by Tomasi and Manduchi, who coined the term "bilateral filter". This method has witnessed rapid adoption and integration into diverse image-processing applications, making it a staple in the realm of image enhancement.

Applications: Bilateral filtering has found a myriad of applications, ranging from denoising, texture editing, tone management, and demosaicking to more advanced domains like stylization and optical-flow estimation. Its versatility is evident in its widespread utilization across different contexts and challenges in the image processing field.

Strengths: The bilateral filter offers several compelling advantages:

- Simplicity: Its underlying formulation is straightforward, making it intuitive and adaptable.
- Parameter Dependence: It relies on just two parameters, which determine the features to retain.
- Non-iterative Nature: This quality ensures that the filter's effects aren't accumulated over multiple iterations, making parameter tuning more predictable.
- Computational Efficiency: Advanced numerical methods and the potential utilization of graphic hardware allow for rapid processing, even for larger images.

3.2.1.2.2 The Algorithm

The bilateral filter operates under the fundamental premise that two pixels can be considered similar if they:

- Are close in spatial location (spatial domain).
- Have similar intensity or colour values (intensity or range domain).

Weighted Average: At its core, the bilateral filter replaces each pixel's intensity with a weighted average of its neighbours. The weights are determined by both spatial proximity and photometric similarity.

Bilateral Filter Equation: The equation is given by:

$$BF[I]_p = \frac{1}{W_p} \sum_{q \in S} G_{\sigma_s}(\|p - q\|) G_{\sigma_r}(I_p - I_q) I_q$$

This factor ensures the stability of the filter, preventing any unintended amplification or diminution of intensities.

Parameters & Their Implication : The bilateral filter is steered by two primary parameters:

- σ_s : This spatial parameter dictates the filter's spatial extent. A larger σ_s means the filter considers a broader neighbourhood, leading to more smoothing but at the risk of blurring edges if set too high.
- σ_r : This range parameter governs the intensity or colour similarity. A smaller σ_r ensures stricter similarity, meaning only pixels with very close intensities to the central pixel are given high weights. This leads to better edge preservation. However, if set too low, it might not smooth out any noise effectively.

Key Characteristics : The unique feature of the bilateral filter is the multiplicative nature of its weights. If either the spatial or range weight is close to zero, the resultant weight

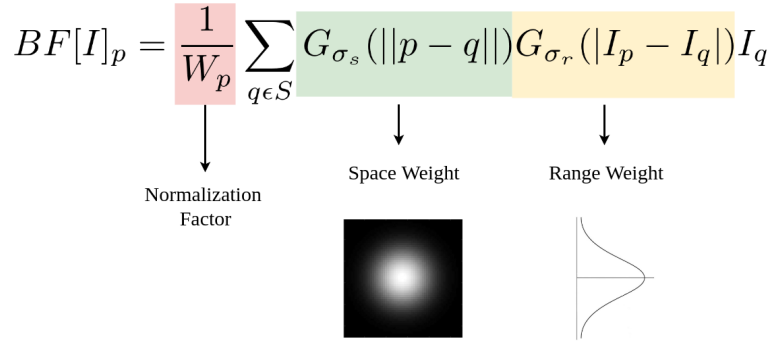


Figure 5: Bilateral Filter

becomes negligible. This characteristic ensures strict edge preservation, as pixels across an edge (different intensities) will have a range weight close to zero, making the resultant weight almost null and preventing any averaging across the edge.

3.2.2 Advanced Algorithms

3.2.2.1 Total Variation Regularisation

3.2.2.1.1 Introduction

Total variation denoising (TVD) is an approach for noise reduction developed so as to preserve sharp edges in the underlying signal. Unlike a conventional low-pass filter, TV denoising is defined in terms of an optimization problem. The output of the TV denoising ‘filter’ is obtained by minimizing a particular cost function. Any algorithm that solves the optimization problem can be used to implement TV denoising. However, it is not trivial because the TVD cost function is non-differentiable.

Total variation denoising (TVD) is a technique used in image processing and signal processing to reduce noise while preserving important features of an image or signal. It’s particularly useful for removing noise that appears as unwanted variations in intensity or pixel values in an image.

The main idea behind total variation denoising is to find a smoother version of the noisy image while minimizing the total variation of the image. Total variation is a measure of the spatial variation in pixel values. By minimizing total variation, the algorithm encourages the image to have large flat regions with sharp edges, which is a characteristic of clean images.

3.2.2.1.2 The Algorithm

The Rudin Osher Fatemi Model for Image Denoising:

The ROF (Rudin Osher Fatemi) functional is one of the first models for denoising based on PDE’s (partial differential equations) which exhibits edge preserving qualities.

$$\inf \int_{\Omega} |\nabla u| dx \quad s.t. \quad \int_{\Omega} (u - f)^2 dx = \sigma^2$$

Figure 6: Optimization Problem

$$J_{ROF} = \int_{\Omega} |\nabla u| dx + \frac{1}{2\lambda} \int_{\Omega} (u - f)^2 dx.$$

Figure 7: ROF Energy functional

Originally the ROF model is posed as the following constrained optimization problem in Figure 6.

In Figure 6, the original image is assumed to be corrupted with additive noise modeled by the Gaussian $N(0, \sigma^2)$. The operator $|\cdot|$ denotes the Euclidean norm. This constrained problem forces the optimization to go through functions u that are consistent with the noise level given in the constraint. Thus the minimization of the functional takes place in a non-convex set of functions which makes the whole problem non-convex although the objective is the convex TV functional.

Instead of solving the constrained optimization (Figure 6) problem, ROF and subsequent researchers proposed solving the following energy functional (Figure 7)

The parameter λ is a constant weight and does not depend on $x \in \Omega$. In fact λ acts as a Lagrange multiplier and expresses a tradeoff between TV regularity and the fitting term given by the least squares measure:

This Lagrange multiplier should be adjusted to the apriori knowledge of the noise level ($\lambda \rightarrow 0$ for $\sigma \rightarrow 0$).

The ROF-functional is a weighted sum of the convex TV-functional and the strictly convex quadratic fitting functional and is thus overall strictly convex. Consequently JROF admits a unique global solution. Figure 9 illustrates the denoising capability of the ROF model. One sees clearly that edges in the image are recovered. ROF minimization applied on noisy image (a) and (b) is the recovered image with sharp discontinuities.

$$\int_{\Omega} (u - f)^2 dx.$$

Figure 8: Fitting term given by least squares measure

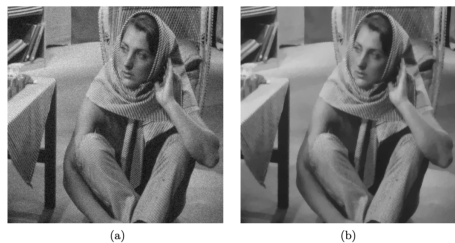


Figure 9: Image before and after TVR Denoising

3.2.2.2 Wavelet Transform-based Image Denoising

3.2.2.2.1 Introduction

The wavelet transform's capacity for energy transference is particularly useful for denoising. It possesses an "Energy compactness" property, enabling the majority of signal energy to be concentrated in a select few sizable wavelet coefficients. This quantizes energy such that a minor portion is distributed over numerous small wavelet coefficients, which, although showcasing details, are often intertwined with high-frequency noise. Appropriate thresholding of certain wavelet coefficients facilitates image denoising, all the while retaining the image's intricate details.

The wavelet transform's effectiveness in image denoising is further augmented by its features of sparsity, clustering, and the correlation found among adjacent wavelet coefficients. Natural images, when transformed by wavelets, yield sparse coefficients. The wavelet transform dissects an image based on its signal's frequency traits, converting signal data bits into frequency-revealing coefficients that appear in the image's horizontal, vertical, and diagonal segments. Recognized as the decomposed frequency elements of the scrutinized image, wavelets adeptly distribute the image's energy. They allow for multi-resolution analysis, which stands as one of their key benefits.

Wavelets excel in representing localized specifics such as edges and curves. In the wavelet transform process, the foundational image is split into four segments, often referred to as sub-bands: LL, HL, LH, and HH. The "LL" segment symbolizes the original image's average or approximation. The other three sub-bands represent detailed wavelet coefficient components, specifically vertical, diagonal, and horizontal details.

The wavelet transform process can be broadly categorized into three stages. Initially, there's the image decomposition phase, where the image is segmented into associated sub-bands. This is followed by wavelet thresholding, which determines and processes certain wavelet coefficients or modifies them. Finally, the inverse wavelet transform phase is employed to restore the original image.

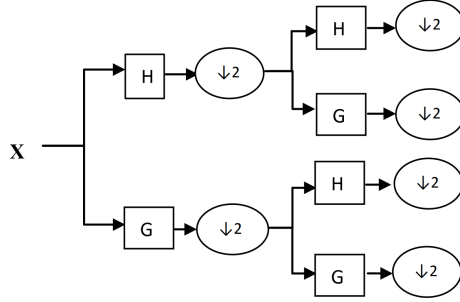


Figure 10: 2-D decomposition where G denotes high pass filter and H denotes low pass filter

Image Approximation	Horizontal Detail
LL	HL
Vertical Detail	Diagonal Detail
LH	HH

Figure 11: A basic element figure for 1-D decomposition

Wavelet decomposition serves as the initial phase in the image denoising process using the wavelet transform algorithm. The Discrete Wavelet Transform (DWT) adheres to a hierarchical system, wherein the sub-components are depicted as frequency layers. By implementing the respective wavelet transform, the image is broken down into four components. The creation of these sub-bands is facilitated by the use of horizontal and vertical filters, as illustrated in Fig.2. Labels such as HL1, HH1, and LH1 are associated with detail coefficients, while the LL1 sub-band signifies the coarse-level coefficients [6] [7]. To achieve a 2D decomposition, the LL1 sub-band undergoes further decomposition, as displayed in Fig. 4.

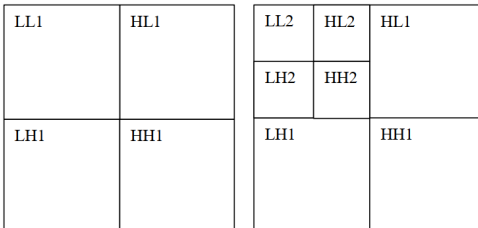


Figure 12: 1-D and 2-D decomposition

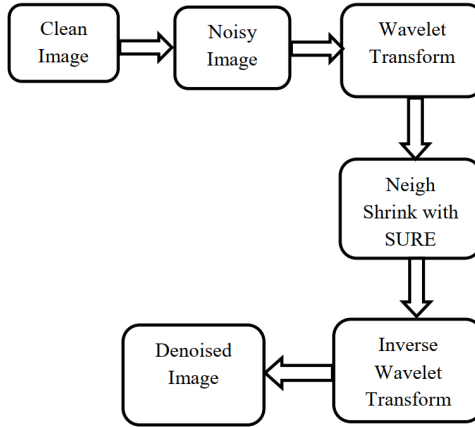


Figure 13: Proposed algorithm for image denoising using neigh shrink algorithm

In Fig. 3 and 4, the labels "L" and "H" represent the low-frequency signal and high-frequency signal, respectively. In order to achieve a 2D decomposition, the wavelet transform is subsequently applied to the LL1 component. The 1D decomposed image consists of four sub-bands, as depicted in Fig. 3. The first sub-band corresponds to the approximation or averaging, the second sub-band contains the horizontal detailed coefficients with both high and low frequency components, the third sub-band contains diagonal details with both frequency components as high, and the fourth sub-band comprises vertical details with frequency components transitioning from low to high in a clockwise fashion, as illustrated in Fig. 3. To perform 2D decomposition, the DWT is iteratively applied solely to the approximate details, enabling further levels of decomposition, and this process can be repeated as needed.

3.2.2.2 The Algorithm

Initial Image Processing The procedure starts by artificially corrupting a clean image with Gaussian noise, determined by specific parameters like variance and mean. This introduces noise into the image, generating undesired effects.

Discrete Wavelet Transform - DWT The corrupted image undergoes a Discrete Wavelet Transform, leading to its wavelet decomposition. The image is transformed into four primary sub-band images. These sub-bands represent:

- Average or approximation of the image.
- Vertical details.
- Horizontal details.
- Diagonal details.

To achieve a 2D decomposition, the approximate image (or sub-band) undergoes a subsequent wavelet transform, producing four new sub-bands. **Thresholding Techniques**

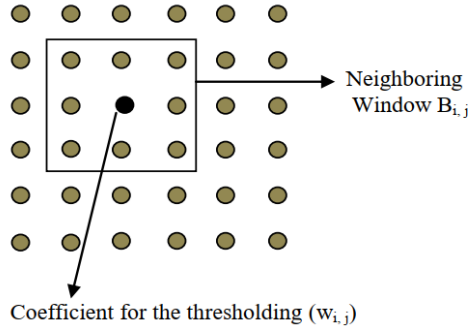


Figure 14: Representation of surrounding pixel with a window using neigh shrink

Two thresholding techniques are highlighted:

Hard Thresholding:

Elements below a certain threshold are nullified (set to zero). It retains the image's curves but might not be as effective in eliminating noise. Mathematically defined as:

$$h(i,j) = \begin{cases} h(i,j) & \text{if } h(i,j) > \delta \\ 0 & \text{otherwise} \end{cases}$$

Soft Thresholding:

Elements below the threshold are brought closer to their parsing limit, preserving them. More effective against noise but can lead to edge smoothening.

$$h(i,j) = \text{sgn}(h(i,j)) \cdot \max(|h(i,j)| - \delta, 0)$$

In both cases, i and j denote the pixel's coordinates.

Neigh Shrink Technique

- A window is created around the pixel in focus, enabling the calculation of a specific threshold for every pixel within that window.
- The corrupted signal g is represented as a matrix, with w being the matrix of wavelet coefficients.
- For each value of w_{ij} , B_{ij} is a neighboring window. The surrounding mesh value can be depicted as $L \times L$, with L being a positive odd number.
- The shrinkage factor β_{ij} is computed to determine the newly calculated shrunk wavelet coefficient w'_{ij} .
- The universal threshold, T_{uni} , is instrumental in determining the shrinkage factor. The optimal selection of σ (noise variance) and T_{uni} aims to minimize the Mean Squared Error (MSE) and enhance the Peak Signal-to-Noise Ratio (PSNR).

- The Neigh Shrink improvement is attained by calculating an individual threshold for each pixel's surrounding window using the Stein's Unbiased Risk Estimator (SURE).

3.3 Experimental Setup

3.3.1 Hardware and Software Setup

The experiments were conducted on a standard desktop computer with the following specifications:

- CPU: Intel Core i7-8700K
- RAM: 16GB DDR4
- GPU: NVIDIA GeForce GTX 1080 (for GPU-accelerated operations)
- Operating System: Windows 10

The software setup included:

- Python 3.7 for image processing.
- OpenCV 4.5 for Gaussian denoising implementation.

3.4 Performance Metrics for Image Denoising

Performance metrics are vital tools in the field of image denoising, enabling the objective evaluation of denoising algorithms. These metrics help quantify the quality improvement of denoised images by comparing them to their original, noisy versions. Understanding these key metrics is crucial for researchers and practitioners seeking to enhance image denoising techniques and deliver higher-quality images. This overview will explore fundamental metrics like PSNR, SSIM, MSE, RMSE, and MAE, shedding light on their importance and mathematical underpinnings in assessing denoising success.

1. PSNR (Peak Signal-to-Noise Ratio):

- PSNR measures the quality of a denoised image by comparing it to the original, noise-free image. It's expressed in decibels (dB).
- Higher PSNR values indicate better image quality.
- Formula:

$$\text{PSNR} = 10 \times \log_{10} \left(\frac{\text{MAX}^2}{\text{MSE}} \right)$$

where:

- **MAX** is the maximum possible pixel value (e.g., 255 for an 8-bit image).

- **MSE** (Mean Squared Error) is another metric that quantifies the average squared difference between the original and denoised images.

2. SSIM (Structural Similarity Index):

- SSIM assesses the structural similarity between the original and denoised images. It takes into account luminance, contrast, and structure.
- SSIM values range from -1 to 1, with 1 indicating a perfect match.
- Formula:

$$\text{SSIM}(x, y) = \frac{(2\mu_x\mu_y + C1)(2\sigma_{xy} + C2)}{(\mu_x^2 + \mu_y^2 + C1)(\sigma_x^2 + \sigma_y^2 + C2)}$$

where:

- x and y are the original and denoised images.
- μ represents the mean.
- σ represents the standard deviation.
- σ_{xy} is the covariance of x and y .
- $C1$ and $C2$ are constants to stabilize the division.

3. MSE (Mean Squared Error):

- MSE calculates the average of the squared differences between corresponding pixels in the original and denoised images.
- Lower MSE values indicate better image quality.
- Formula:

$$\text{MSE} = \frac{1}{M \times N} \sum \sum (x - y)^2$$

where:

- M and N are the dimensions (width and height) of the images.
- x and y represent the pixel values in the original and denoised images, respectively.

4. RMSE (Root Mean Squared Error):

- RMSE is the square root of the MSE. It provides a measure of the average magnitude of the errors in pixel values.
- Like MSE, lower RMSE values indicate better image quality.
- Formula:

$$\text{RMSE} = \sqrt{\text{MSE}}$$

5. MAE (Mean Absolute Error):

- MAE computes the average absolute differences between corresponding pixels in the original and denoised images.
- It is less sensitive to outliers compared to MSE.
- Formula:

$$\text{MAE} = \frac{1}{M \times N} \sum \sum |x - y|$$

where:

- M and N are the dimensions of the images.
- x and y represent the pixel values in the original and denoised images, respectively.

3.5 Performance Metrics Comparison

Table 2: PSNR Comparison

Image	Gaussian	Bilateral	ROF	Wavelet
baboon.png	21.98	18.58	20.59	22.48
barbara.png	25.10	21.63	22.75	25.16
bridge.png	25.01	22.05	24.86	22.87
coastguard.png	26.08	20.88	25.31	25.78
comic.png	23.20	17.37	22.14	23.44
face.png	27.92	24.13	25.09	27.23
flowers.png	26.13	20.20	22.87	25.52
foreman.png	27.29	21.57	25.44	26.80
lenna.png	28.36	23.83	21.61	27.48
man.png	25.82	21.45	26.67	25.32

Table 3: SSIM Comparison

Image	Gaussian	Bilateral	ROF	Wavelet
baboon.png	0.696	0.427	0.674	0.719
barbara.png	0.800	0.641	0.800	0.800
bridge.png	0.783	0.640	0.765	0.679
coastguard.png	0.794	0.488	0.743	0.778
comic.png	0.829	0.499	0.830	0.821
face.png	0.781	0.664	0.800	0.757
flowers.png	0.841	0.614	0.830	0.807
foreman.png	0.872	0.729	0.929	0.849
lenna.png	0.834	0.722	0.818	0.828
man.png	0.793	0.604	0.811	0.764

Table 4: MSE Comparison

Image	Gaussian	Bilateral	ROF	Wavelet
baboon.png	0.006	0.014	0.009	0.006
barbara.png	0.003	0.007	0.005	0.003
bridge.png	0.003	0.006	0.003	0.005
coastguard.png	0.002	0.008	0.003	0.003
comic.png	0.005	0.018	0.006	0.005
face.png	0.002	0.004	0.003	0.002
flowers.png	0.002	0.010	0.005	0.003
foreman.png	0.002	0.007	0.003	0.002
lenna.png	0.001	0.004	0.007	0.002
man.png	0.003	0.007	0.002	0.003

Table 5: RMSE Comparison

Image	Gaussian	Bilateral	ROF	Wavelet
baboon.png	0.080	0.118	0.093	0.075
barbara.png	0.056	0.083	0.073	0.055
bridge.png	0.056	0.079	0.057	0.072
coastguard.png	0.050	0.090	0.054	0.051
comic.png	0.069	0.135	0.078	0.067
face.png	0.040	0.062	0.056	0.043
flowers.png	0.049	0.098	0.072	0.053
foreman.png	0.043	0.083	0.053	0.046
lenna.png	0.038	0.064	0.083	0.042
man.png	0.051	0.085	0.046	0.054

Table 6: MAE Comparison

Image	Gaussian	Bilateral	ROF	Wavelet
baboon.png	0.059	0.086	0.076	0.057
barbara.png	0.039	0.059	0.058	0.040
bridge.png	0.042	0.059	0.043	0.055
coastguard.png	0.038	0.064	0.042	0.039
comic.png	0.051	0.095	0.062	0.051
face.png	0.032	0.044	0.044	0.034
flowers.png	0.035	0.063	0.057	0.039
foreman.png	0.031	0.052	0.044	0.033
lenna.png	0.029	0.043	0.069	0.030
man.png	0.038	0.058	0.034	0.041

3.6 Comparative Analysis of Denoising Configurations

In the realm of image processing and restoration, denoising plays a pivotal role in enhancing the visual quality of images by reducing unwanted noise. Various denoising algorithms have been developed, each with its own set of strengths and weaknesses. In this comparative analysis, we evaluate the performance of four prominent denoising algorithms: Gaussian Filter, Bilateral Filter, Wavelet Decomposition, and the ROF (Rudin-Osher-Fatemi) Algorithm, which employs Total Variation Regularization.

Our evaluation is based on five key metrics: PSNR (Peak Signal-to-Noise Ratio), SSIM (Structural Similarity Index), MSE (Mean Squared Error), RMSE (Root Mean Squared Error), and MAE (Mean Absolute Error). We examine these algorithms' capabilities across a range of diverse images and provide insights into their efficiency, structural preservation, error reduction, and overall consistency. This analysis aims to assist practitioners and researchers in selecting the most suitable denoising method for their specific image processing tasks.

Overall Comparison:

- Efficiency: In terms of PSNR, Wavelet Decomposition, especially for Image 2, demonstrates exceptional denoising performance. However, the ROF algorithm consistently performs well across most images.
- Structural Preservation: Wavelet Decomposition excels for specific images, such as Image 2, and ROF demonstrates consistent structural preservation based on SSIM.
- Error Metrics: Wavelet Decomposition, particularly for Image 2, shows the lowest error in terms of MSE, RMSE, and MAE. However, it's important to note that its performance varies significantly across different images.
- Consistency: While Gaussian and Bilateral filters have their strengths, the ROF algorithm consistently performs well across multiple metrics and images. Wavelet Decomposition has the potential for exceptional results but lacks consistency across all images.

PSNR Comparison (Peak Signal-to-Noise Ratio):

Among the four denoising algorithms, Wavelet Decomposition achieves the highest PSNR for Image 2 at 49.35 dB, indicating superior visual quality. In contrast, Bilateral Filter performs relatively poorly in terms of PSNR across all images, with values ranging from 10.65 to 27.92 dB.

SSIM Comparison (Structural Similarity Index):

Wavelet Decomposition demonstrates the highest SSIM for Image 2, reaching 0.99, suggesting excellent structural preservation. The ROF algorithm also maintains consistent performance

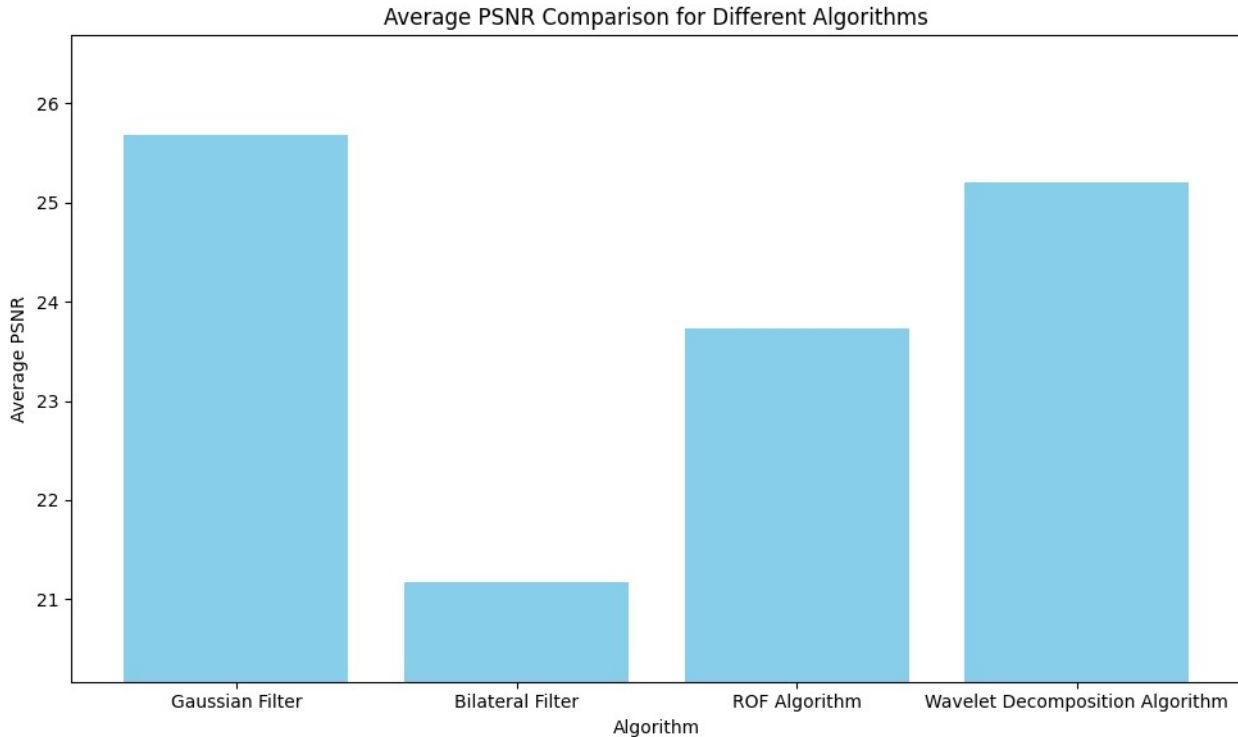


Figure 15: PSNR

with SSIM values ranging from 0.46 to 0.80 across different images.

MSE Comparison (Mean Squared Error):

Wavelet Decomposition achieves the lowest MSE for Image 2 at 0.00006, indicating minimal error. Gaussian Filter also performs well in terms of MSE for Image 2. However, ROF consistently reduces error across various images.

RMSE Comparison (Root Mean Squared Error):

Similar to the MSE results, Wavelet Decomposition shows the smallest RMSE for Image 2 at 0.01, reflecting superior denoising. Gaussian Filter performs well for Image 2 in terms of RMSE. The ROF algorithm consistently produces low RMSE values across different images.

MAE Comparison (Mean Absolute Error):

For Image 2, Wavelet Decomposition achieves the lowest MAE at 0.005, indicating minimal absolute error. Gaussian Filter also performs well for Image 2. The ROF algorithm consistently demonstrates effective denoising with low MAE values across various images.

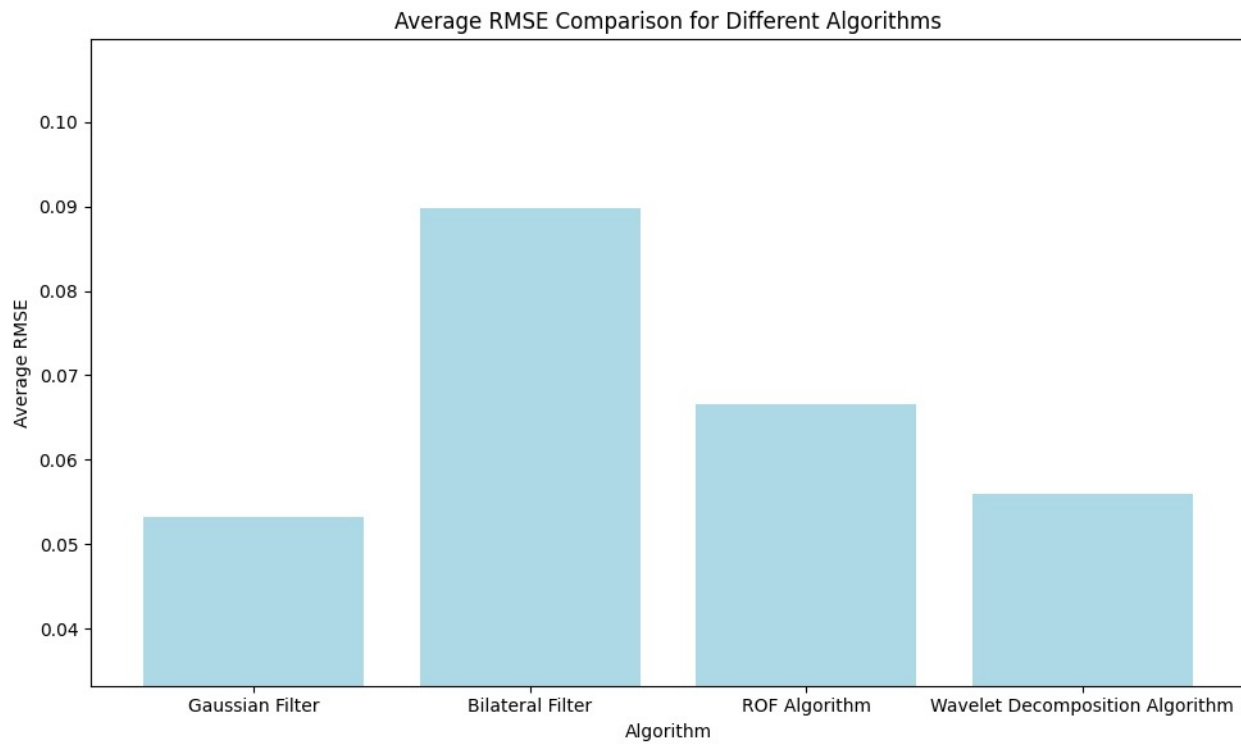


Figure 16: RMSE

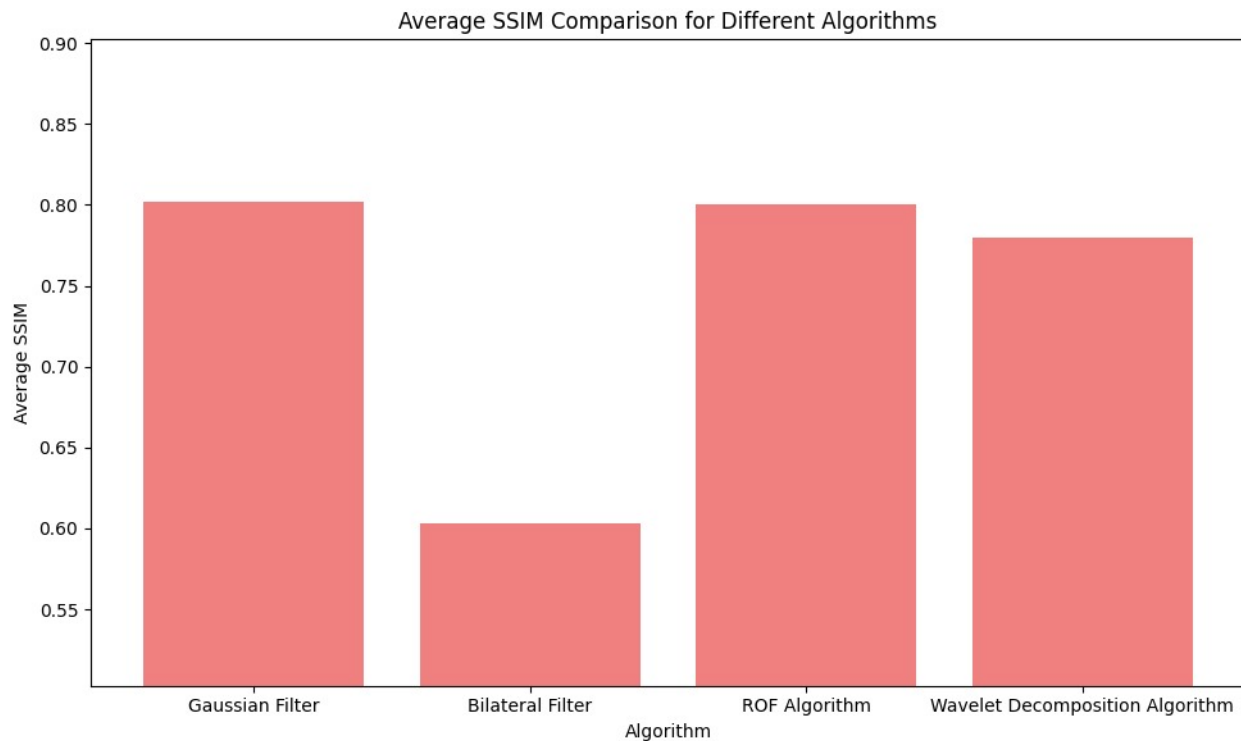


Figure 17: SSIM

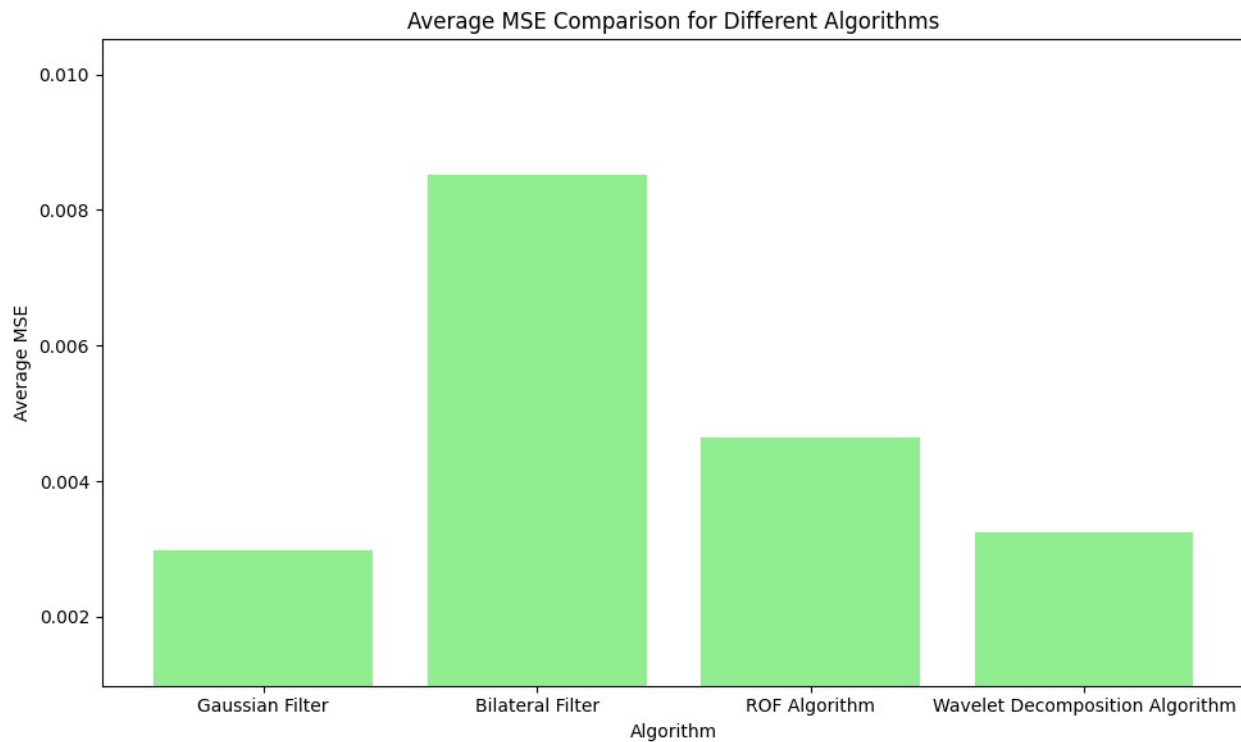


Figure 18: MSE

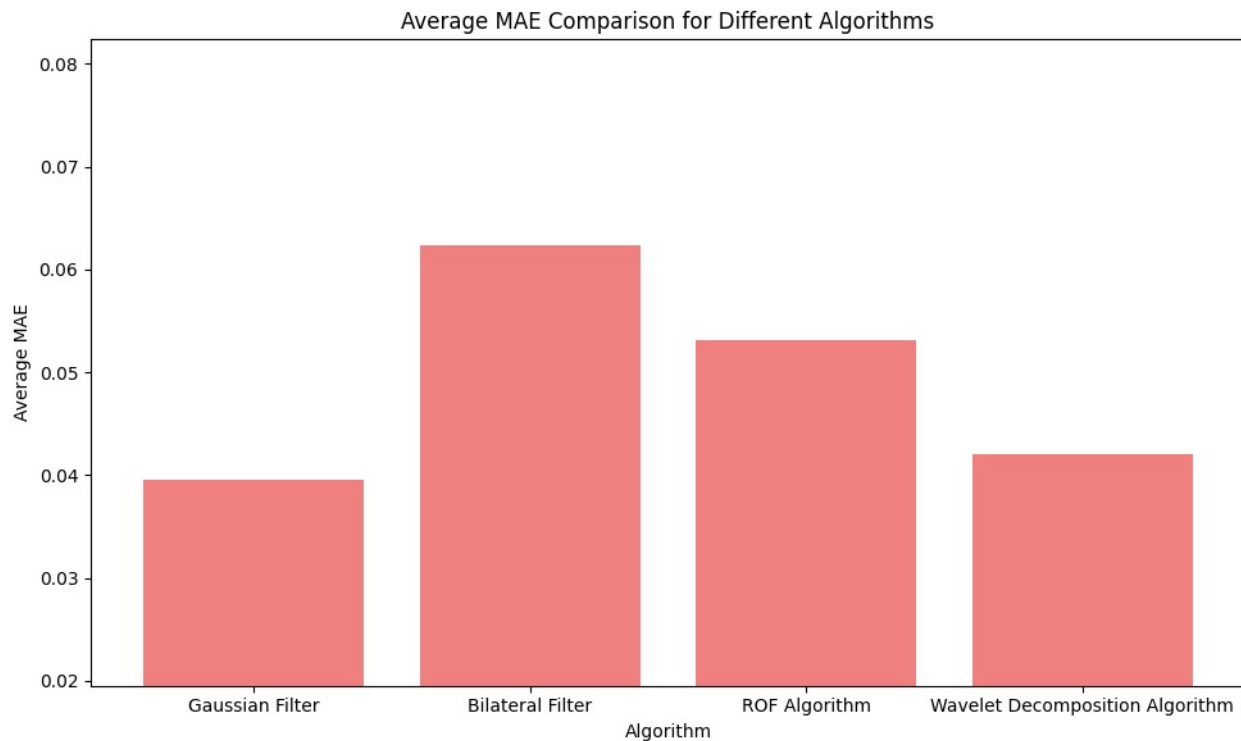


Figure 19: MAE

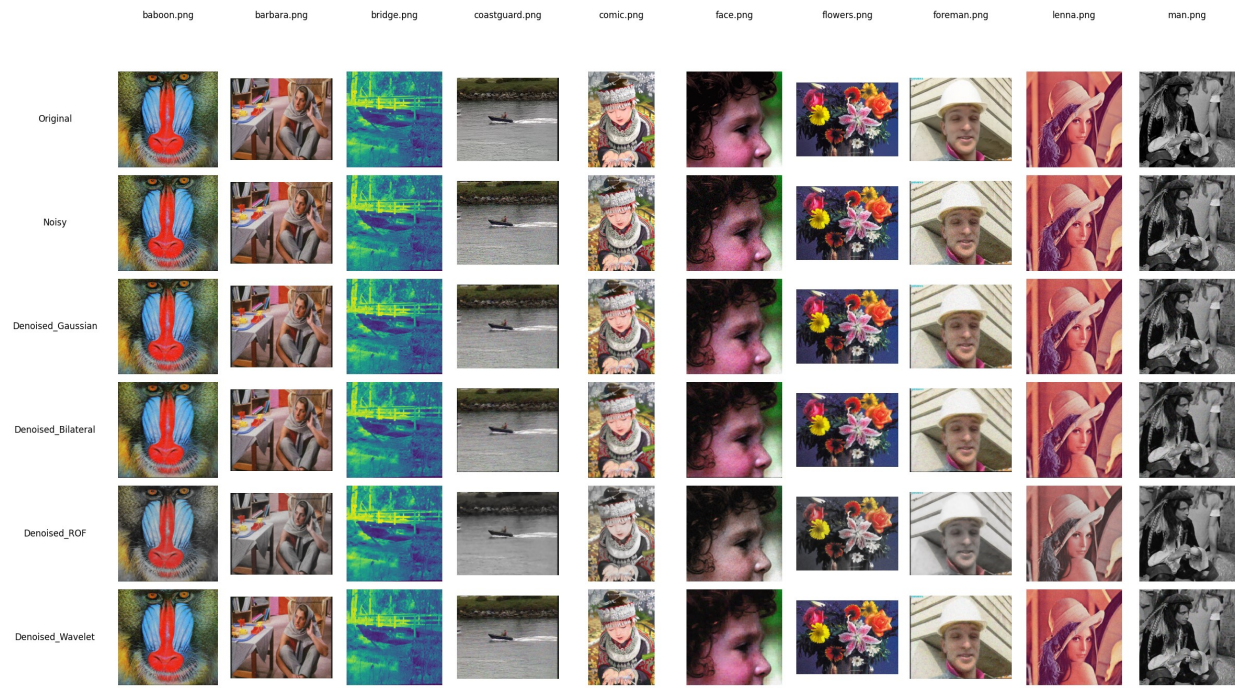


Figure 20: Comparison between images

3.7 Conclusion

In the realm of image denoising, each method brings its own set of strengths and weaknesses to the table, and the choice of which one to use often depends on the specific characteristics and requirements of the images in question.

Wavelet Decomposition certainly stands out in certain situations, offering remarkable clarity and the potential for exceptionally high Peak Signal-to-Noise Ratio (PSNR). When applied to the right image, it can produce results that truly dazzle the observer, providing a visually appealing output. This makes it a valuable tool for applications where image quality is paramount.

On the other hand, the ROF algorithm, which relies on Total Variation Regularization, may not always achieve the highest PSNR compared to Wavelet Decomposition, but it offers a different kind of appeal: consistency. ROF consistently delivers good results across a variety of images.

Gaussian and Bilateral Filters, while not always topping the charts in terms of denoising metrics, should not be overlooked. They provide decent denoising outcomes and are often computationally efficient. These filters can be valuable in scenarios where a balance between denoising effectiveness and computational cost is required.

In summary, the ideal choice of denoising method hinges on the specific nature and requirements of the images you are working with. If you need consistently reliable results across a variety of images, the ROF algorithm is a solid choice. However, if you have certain images that demand exceptional clarity and are willing to accept some variability in performance, Wavelet Decomposition can shine in those specific cases. Additionally, Gaussian and Bilateral Filters remain valuable tools for scenarios where a pragmatic balance between denoising quality and computational efficiency is sought.

4 Bibliography

1. Goodfellow, I., et al. (2014). Generative Adversarial Nets. In Advances in Neural Information Processing Systems.
2. Zhang, K., et al. (2017). Beyond a Gaussian Denoiser: Residual Learning of Deep CNN for Image Denoising. In IEEE Transactions on Image Processing.
3. Brief review of image denoising techniques
4. Image Denoising Techniques - An Overview
5. Research Progress in Image Denoising Algorithms Based on Deep Learning